PROGRESS IN THE DEVELOPMENT OF ELECTRO STATIC DEFLECTION

bу

Kurt Schlesinger

TV Research Department Motorola Inc. Chicago, Illinois

INTRODUCTION

Considering the continued improvement of our technique of magnetic deflection, progress in the development of electrostatic deflection appears slow by comparison. It appears, that the electrostatic approach is up against two major difficulties:

- 1. High deflection voltage demand.
- 2. Relatively high deflection aberrations.

The voltage demand is in direct proportion to beam voltage, and increases with the square of the tangent of the sweep half-angle. It equals anode potential at a design-angle of 54°, doubles it at 72°. This fact, plus severe problems of insulation have precluded the use of e.-s. deflection for "stiff" beams at the high ultor voltages now in use. (15 • 30 KV)

Deflection defects, such as defocussing, spot and pattern distortion, are worse than with magnetic deflection and increase rapidly with angle, at least in conventional deflection units. This has limited e.-s. sweep to narrow angle applications, such as oscilloscopes. (\$\omega \le 25^\circ{0}\).

Recently, two developments have taken place, which, in combination, may make further progress possible. One is the development of electrostatic yokes which permit bi-axial deflection from a common center with much less scan distortion, and at wider angles than previously possible. The other is the advent of the mask-type intensifiers which permit a high order of post-acceleration without loss of deflection. Both developments will be discussed in the following paper.

I. The Electrostatic Yoke

Early work on the electrostatic yoke or "Deflectron", has been reported (a) previously. The basic principle is briefly reviewed with aid of Figure (1). Two voltages V_x and V_y , both balanced to ground, are applied to four separate electrodes, printed on the inside of a cylinder. The pattern geometry is of a design such that the effective wall potential ϕ seems to vary sinusoidally with angle:

$$\phi_{R,a} = \# \left[\frac{1}{2} V_{y} \sin A + \frac{1}{2} V_{x} \cos A \right] ; K < I$$
 (1)

The potential on the inside then becomes

$$\mathcal{L}_{\mathbf{r},\mathbf{x}} = \mathcal{L}_{\mathbf{R},\mathbf{x}} \cdot \frac{\mathbf{r}}{\mathbf{R}} = \frac{K}{2R} \left[V_{\mathbf{y}} \cdot \mathbf{y} + V_{\mathbf{x}} \cdot \mathbf{x} \right]$$
 (2)

The fields in x and y direction are the respective gradients of (2)

$$E_{\chi} = \frac{\partial Y}{\partial \chi} = K \frac{\forall \chi}{2R}$$

$$E_{\chi} = \frac{\partial Y}{\partial \chi} = K \cdot \frac{\forall \chi}{2R}$$
(3)

This is the same field as would be produced by two cressed pairs of plates bounding the cylinder, each connected to a voltage of KV_x and KV_y respectively. It will be shown below (eq. 7) that K has the value 0.707. This is the relative sensitivity of the "Deflectron" compared to the equivalent plates. However, while the equivalent capacitors cannot operate unless arranged sequentially along the beam, the electrostatic yoke can perform bi-axial deflection simultaneously, i.e., with a common center for both coordinates. This saves two to one in overall length and offers other advantages as well.

II. Printed Circuit Geometry for Electrostatic Yokes

Figure 2 shows the pattern geometry of an electrostatic yoke, evolved into

a plane. The pattern has double periodicity, namely four cycles to the perimeter and three or four cycles (\land) along the length of the cylinder. All boundaries shown are halfwaves of $\sin \land$ offset by a small "dead-angle" $\pm \land$ at the starting point, to provide insulation. The various boundaries are thus formulated by:

$$\Lambda \cdot \frac{1 \pm \sin(\alpha \pm \Delta)}{2}$$
 and $\Lambda \cdot \frac{1 \pm \cos(\alpha \pm \Delta)}{2}$ (4)

in a sequence as indicated on Figure 2.

To predict the performance of this device, we assume two equal and balanced deflection voltages:

$$V_x = \cos \omega t$$
 $V_y = \sin \omega t$ (5)

to be connected to the four metal stripes as shown in Figure 2. Across the insulating interfaces we assume the potential to vary linearly from one boundary to the other. Limiting ourselves to one wavelength λ as unit length, the effective potential is found in the interval: $\pm \Delta \leq \alpha \leq \frac{\pi}{2} - \Delta$ surrounding the N-axis, by summing up the following terms:

Effective Length	Potentia1
1 - 1+ sin (x+A)	-coswt
+ Sin (x-A) 1+ cos(x+4) 2) + sin wt
1-005 (x-4)	+ cos wt
$\frac{1+\sin(\alpha+4)}{2} \frac{1+\sin(\alpha-4)}{2}$	1 -eoswt + sinw
$\frac{\cos(\alpha+\Delta)}{2} = \frac{1-\cos(\alpha-\Delta)}{2}$	sinut + cosu
	$ \begin{array}{c ccccccccccccccccccccccccccccccccccc$

The end result of this calculation is as follows:

æg. #	Zone	Effective Potential	
(6a)	Metallized areas	$\phi_m = 0.707 (\cos A - \sin A) \sin (\alpha + \omega t - \frac{\pi}{4})$	
(6b)	Glass interfaces	$\phi_g = 0.707$, $\sin \Delta \cdot \sin (\alpha + \omega t - \frac{\pi}{4})$	
(6c)	Resulting total axial potential	$ \varphi_a = 0.707 \cdot \cos a \cdot \sin \left(\alpha + \omega t - \frac{\pi}{4} \right) $	

This result is interesting in several respects:

- 1. It indicates the establishment of a uniform rotating field, moving counter-clockwise at uniform angular velocity ...,
- 2. It informs that the electrical axis lie at multiples of 45° off the axis of pattern symmetry, as shown in Figure 2.
- 3. It indicates that the sensitivity of a cylindrical yoke of this type is, for each axis:

times the sensitivity of an equivalent pair of plates touching it.
Since the deflection factor of parallel plates can be written as follows:

$$S_p = 35 \cdot \frac{d}{\ell}$$
 (volts per degree per KV) (8)

the corresponding figure for the Deflectron is:

$$S_d = 50 \cdot \tilde{e} \qquad \text{(volt/kV/deg.)} \tag{9}$$

Each terminal gets one half of this voltage in push-pull operation.

The dead-angle \triangle in Figure 2 is usually smaller than 18 degrees (cos 18° = 0.95). Hence it is safe to say that the sensitivity of a practical Deflectron unit, taken per axis, is two-thirds of a pair of deflection plates of the same length, tangent to it. The same statement holds for conical units as well (see section III).

Figure 3 shows equipment to detect the electrical axis on a finished Deflectron unit. The unit is energized by a balanced 3 mc signal at two opposite terminals.

The two other segments are grounded. A probe with two blades under 90° is inserted into the Deflectron. A null detector indicates the position of the axis of deflection within less than one degree.

III. Deflectron Sensitivity

Figure 4a-b shows two types of electrostatic yokes produced by photoengraving methods on the inside of glass cylinders and cones. The large unit has a diameter ratio m * 4:1 (taper-ratio). The structural and electrical characteristics are given in the following table:

TABLE I

Fig.	Unit	Length	Exit Diameter	Aper Physical	ture Usable	Deflection Factor in volts per deg. per KV. (each terminal)
4а	Pencil Deflectro	n 1½"	<u>1</u> 111	33°	27 ⁰	9•2
4ъ	Cone Deflectron	2"	1 - 3/8"	66°	50°	9.8

The measured sensitivity is in agreement with the theoretical data for a conical yoke with taper ratio m (see appendix):

$$5 = 25 \cdot \tan \frac{\Delta}{2} \cdot \frac{1 - \frac{1}{m} \left[volt/kv/deg \right]}{\epsilon_m m} \left[volt/kv/deg \right]$$
 (10)

They also check with the more convenient approximate formula:

$$S = 25 \cdot \frac{dm}{e} \left[V/KV/deg \right]$$
 (10a)

which holds for any unit with mean diameter d_m and length 1 regardless of taper (15% accuracy up to m = 4).

It is noteworthy that the sensitivity of both units is practically the same, despite the fact that the large unit handles twice as much deflection as the small one. This is in line with a general rule, (see appendix),

whereby the transition from a parallel to a tilted structure has no first order effect on sensitivity, as long as mean diameter and length are unaltered. However, since the exit aperture increases in the process, a conical unit has always greater overall merit than the cylinder. The small pencil—Deflectron is thus recommended only in cases where space is at a premium.

IV. A 12 Inch "Deflectronized" Cathode Ray Tube

Figure 5 shows a gun assembly carrying a conical electrostatic yoke.

(c)

Figure 6 shows a finished tube using this system. This tube employs a 12"

blank as used in the 12LP4 type TV picture tube, to which a funnel section and

2" neck has been added. One stage of post acceleration is used at a voltage

step-up of 1.5:1. (7.5KV at the screen, 5KV in the deflecting space). Full

scan occurs at 50 degrees of deflection which requires 2300 volt peak to peak

at each Deflectron terminal. In this operation, 75% of the yoke aperture can

be utilized, or one-half of the yoke window area, before scan distortion

occurs. This compares favorably with operation of magnetic deflection yokes.

V. Performance Test Station

Figure 7 shows a test set-up to check the performance of the finished tubes. The bulb is mounted vertically in the lower section which contains equipment for circular sweep. The signal generator is carefully filtered and employs inverse feedback to insure sweep waveforms with less than 1% distortion.

An ultra-violet light source projects, onto the screen, the image of a reference chart in polar coordinates. Since the yellow component of the P-7 phosphor responds to UV, we observe, on the screen, the superposition of the reference and the circular scan. Since both displays are in the same plane, the image can be viewed from any point without parallax.

VI. The Circularity Problem

Figure 8 shows a photograph obtained, with the above station, from one

of the earlier tubes. At a sweep diameter of 10" (46 degrees), it is seen that deflection at \pm 45° off axis (diagonal) is slightly larger than on axis. This non-circularity amounts to about 1/8" radial, i.e. $2\frac{1}{2}$ % of the diameter. The error distribution is quadrantal, i.e. repeats itself four times per revolution.

It is possible to account for this quadrantal error by further analysis of the pattern geometry of Figure 2.

To this end, the computation of the effective boundary potential, carried out above for the axial region (Eq. 6a-6c), has been repeated for the diagonal region: $\frac{\pi}{2} - \Delta \leqslant \sqrt{\frac{\pi}{2}} + \Delta$

Calling $\phi_{\mathtt{a}}$ the axial potential, as computed above (Eq. 6c),

we find, by the same methods, an expression for the diagonal potential

$$\phi_{\Delta} = \cos \omega t \frac{1-\sin \alpha - \Delta}{4} + \sin \omega t \frac{1-\sin \alpha + \Delta}{4}$$
 (11)

eq. (11) indicates that diagonal deflection is slightly greater than axial deflection because of the error term $\frac{d}{4}/\frac{d}{d}$. This term can be evaluated at the diagonal points of sweep by setting $\omega t = \frac{\pi}{4}$ in eq. (11) The result is:

 $\phi = 0.707. \Delta^{2}$ (12)

That is, the error increases with the square of the dead angle Δ . Taking the value ϕ_a for axial potential from Θ_a . (6c), we find the quadrantal error percentage:

$$\frac{D-A}{A} = \frac{\phi_{\Delta}}{\phi_{A}} = \frac{\Delta^{2}}{4 \cdot \cos \Delta} \qquad \rho \sim \left(\frac{\Delta}{2}\right)^{2} \cdot 100^{\circ} / o \tag{13}$$

This theoretical non-circularity is evaluated in Table II for three values of dead angle Δ . It is seen, that the theory gives a quantitative account for experience.

TABLE II

Dead Angle	Quadrantal Error	Correcting tabs Height		
12°	1.1%	6 mils		
15°	1.7%	17 mils		
18° 2•5%		25 mils		

VII. Correction of Quadrantal Error

A cure for non-circularity suggests itself by inspection of expression (9) for the error term ϕ_A . The factors $\frac{1-\sin y-A}{4}$ and $\frac{1-\sin y+A}{4}$ in this equation describe the triangular areas shown at x in Figure 2 but in one half of their actual height. It seems possible therefore, to cancel the error term ϕ_A by printing additional tabs of similar shape right above the dead angles $\pm A$ of the pattern, and then connecting these tabs to signals of opposite polarity. This can be done readily in a pattern with an odd number of cycles, such as shown in Figure 2 for N = 3. The required compensating voltages $(-\sin x)$ and $(-\cos x)$ are then easily accessible on adjacent stripes. The height of the compensating tabs may be found from eq. (11).

$$\tilde{R} = \frac{\Delta^2}{8} \cdot \ell \tag{14}$$

where \(\ell \) is the total length of the Deflectron pattern. This strip-width h of the tabs is listed in Table II and it is found to be quite small (approximately 20 mils). Even this small strip-width accrues only if the error is allowed to add up, without correction, over all cycles of the pattern. The sum total is then corrected by tabs at input and output of the yoke.

The photograph, Figure 9, has been taken of one of the early Deflectrons compensated in that manner. It indicates that the quadrantal error has

actually been over-compensated, the diagonals now being about 2% shorter than the axials (D/A \angle 1). Further refinements in our printing technique will undoubtedly permit a more precise correction of residual non-circularity.

VIII. Progress in the Technique of Post Acceleration

Since the voltage demand for electrostatic deflection is directly proportional to the electron-voltage in the deflecting region, any progress in the technique of post acceleration is a great help in the development of electrostatic deflection.

Conventional post-accelerators, also called intensifiers, operate with conductive coatings of band - or spiral shape, plated on the inside of the bulb. In all of these accelerators, including the constant-gradient type, electron trajectories are not straight, but are bent back towards the axis. This causes considerable deflection loss (see Figure 10a) partly offsetting the desired gain from post-acceleration. Another disadvantage of curved trajectories is the need to handle, in the deflecting unit, sweep angles in excess of those finally achieved. This increases deflection distortion in the yoke and forces a reduction of its ultimate efficiency by design.

In 1950, L. S. Allard published, in England, a paper on an "ideal" (d) accelerator for CRT's. He proposed a mask-and-screen assembly to achieve acceleration in a confined region close to the screen (see Figure 10b). Since this arrangement uses most of the bulb as a field-free drift space, trajectories are straight lines and deflection loss may be avoided entirely.

When experimenting with the mask-type of intensifier, we soon came to realize that the major, perhaps the only, obstacle was secondary emission (S.E) from the mask. Figure 11-a shows the pictorial effects of S.E. observed. In these studies, we used a high transmission (50%) mask of copper nickel alloy, one inch away from the screen. The "ghost" image was comparable in brightness to the primary image, but was lagging behind it in deflection

because of beam refraction in the plane mask-and-screen arrangement. Figure 11b shows the same pictures after cancellation of secondary emission. This improvement was obtained by a device, which we call a "barrier-mask" and which is explained in Figure 12.

The inside surface of the intensifier-mask is coated with an insulating material having a high degree of secondary emission. The outer surface is left metallic and is connected to an external bias 100 volt below drift space potential. When scanned, the insulating face soon adopts the potential of the drift space wall, while the second surface acts as a repeller, or "barrier", against secondary emission from the mask.

With this "barrier-mask intensifier", post acceleration of 10:1 has been achieved readily. The portent of this development for electrostatic deflection lies in a considerable reduction of sweep voltage. In experimental tubes, deflection of a 20 KV beam by 62 degrees was done with only 1300 V per plate, using a conical deflectron as shown in Figure 4b. The same sweep would have required 8300 volt per plate with/one-step ring accelerator 1.5:1.

The 12" tube, shown in Figure 6, will sweep 50 degrees at 7.5KV with only 500 V per terminal, if equipped with barrier mask acceleration 10:1. This is only 20% of the voltage which we need now in connection with a conventional ring-accelerator.

In summing up, it appears at this time, that the combination of the Deflectron-yoke with the barrier mask intensifier presents a system for electrostatic deflection, which combines low distortion at wide angles with compactness, and has the ability to scan high ultor voltages with low deflection voltage. Work is under way to use this approach for high intensity CRT's, both (e) in the fields of specialty tubes , as well as for television picture displays.

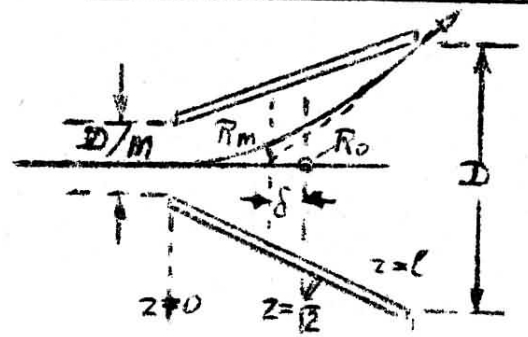
PIBLIOGRAPHY

- (a) Kurt Schlesinger:
 "Internal Electrostatic Deflection Yokes"
 Electronics, July 1952
- (b) V. K. Zworykin, G. A. Morton, E. G. Ramberg, J. Hillier and A. W. Vance:
 "Electron Optics and the Electron Microscope"
 John Wiley, New York, 1945 Chapter XI.
- (c) Built for use in a Radar-Indicator Under Bureau of Ships Contract
- (d) L. S. Allard:
 "An 'Ideal' Post Deflection Accelerator CRT".

 Electronic Engineering, November 1950 pg. 461-463
- (e) This work is done in partial fulfillment of a contract with the U. S. Army Signal Corps.

APPENDIX

Sensitivity Gain Through Taper



We compare a pair of parallel plates to a pair with taper. The taper

factor is m. The plate separation of the tapered pair is:

$$d = \frac{D}{m} \left[1 + (m-1) \cdot \frac{Z}{e} \right] \tag{1}$$

The active field strength then becomes:

$$E_z = E_1 \cdot \frac{1}{1 + (m-1)^2/e}$$
 (2)

where

$$E_{l} = \frac{ed}{D} \cdot m \tag{3}$$

From electron ballistics, we get for the trajectory:

$$\frac{d^2y}{dz^2} = \frac{Ez}{2\phi_a} \tag{4}$$

where of is the voltage of the anode preceding the deflector.

By integration of (2), we get the exit angle of the beam:

$$\frac{dy}{dz_{(2=e)}} = \frac{e_1}{2\phi_2} \cdot \frac{e}{D} \cdot \frac{m \cdot \ln m}{m-1}$$
 (5)

The underlined term is the value for parallel plates. The remaining factor is the reciprocal of taper gain, as used in the report.

For a cone with a 4:1 taper ratio, as shown in Figure 4b, the taper gain is 1/0.545 = 1.83.

Since the approximation:

$$g_{T} = \frac{1 - \frac{1}{m}}{e_{n} m} \sim \frac{1}{2} \left[1 + \frac{1}{m} \right] \tag{6}$$

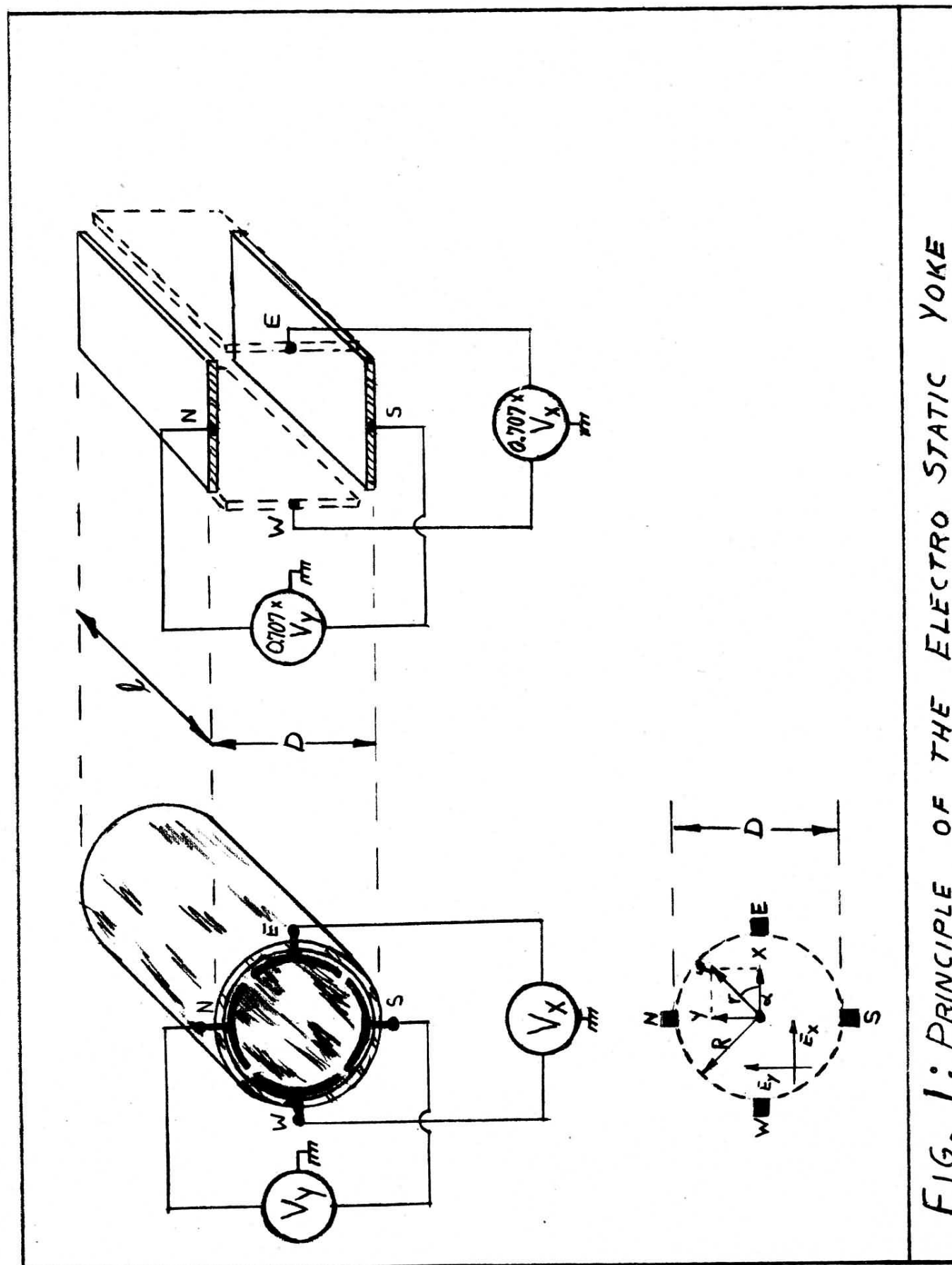
holds within 10% up to m = 3.5, the invariance of sensitivity for units with

equal mean diameter follows.

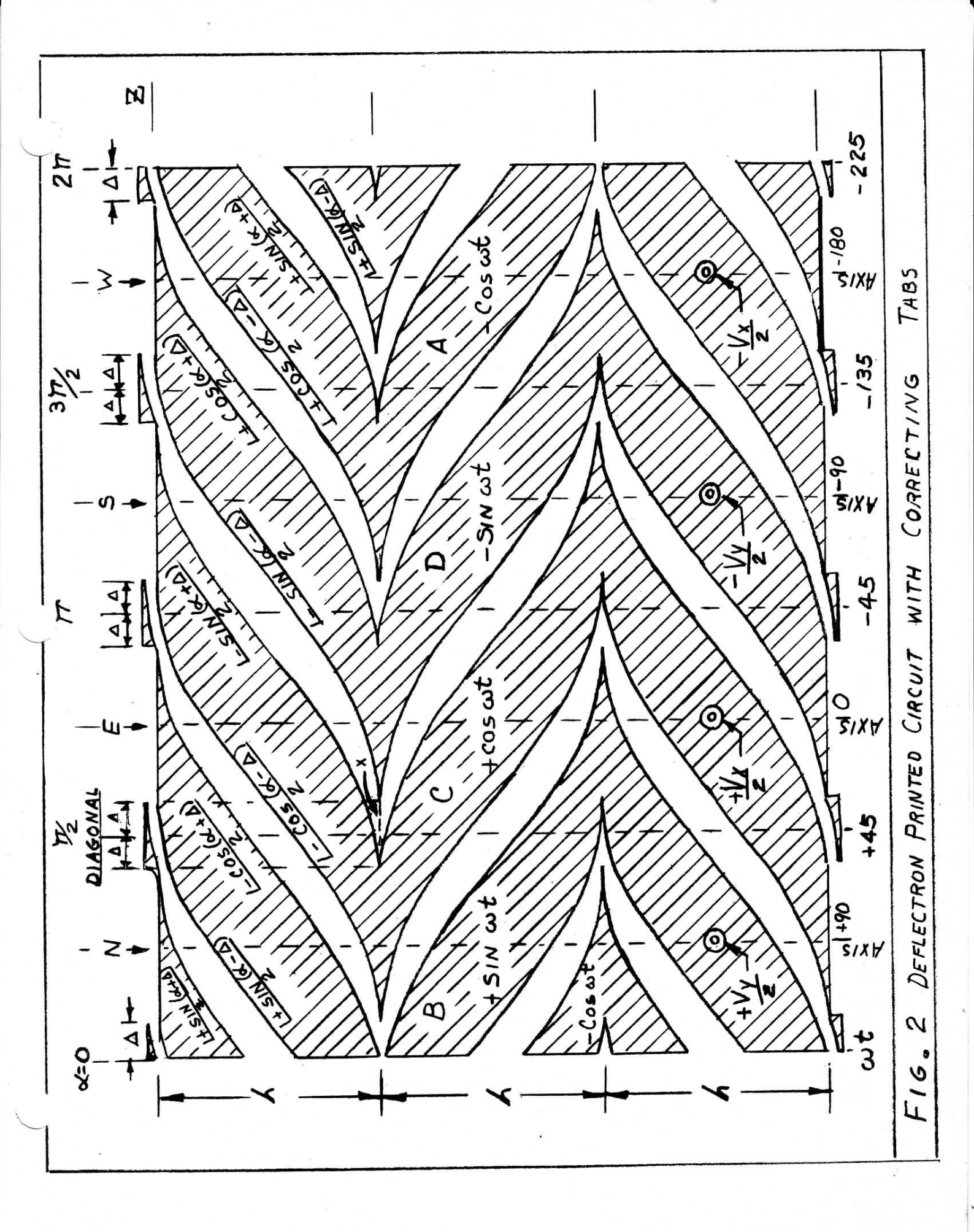
There is a slight reduction of aperture from tapering. The center of rotation R_{m} moves back from the geometrical center of the electrode by the amount Δ :

$$\frac{\delta}{\ell} = \frac{1}{2} \frac{m+1}{m-1} - \frac{1}{\ell m m}$$
 (7)

At a taper-factor of m = 4, as used in our Deflectrons, this shift is 11% of the total length of the electrode.



ELECTRO STATIC THE 40 FIG. 1: PRINCIPLE



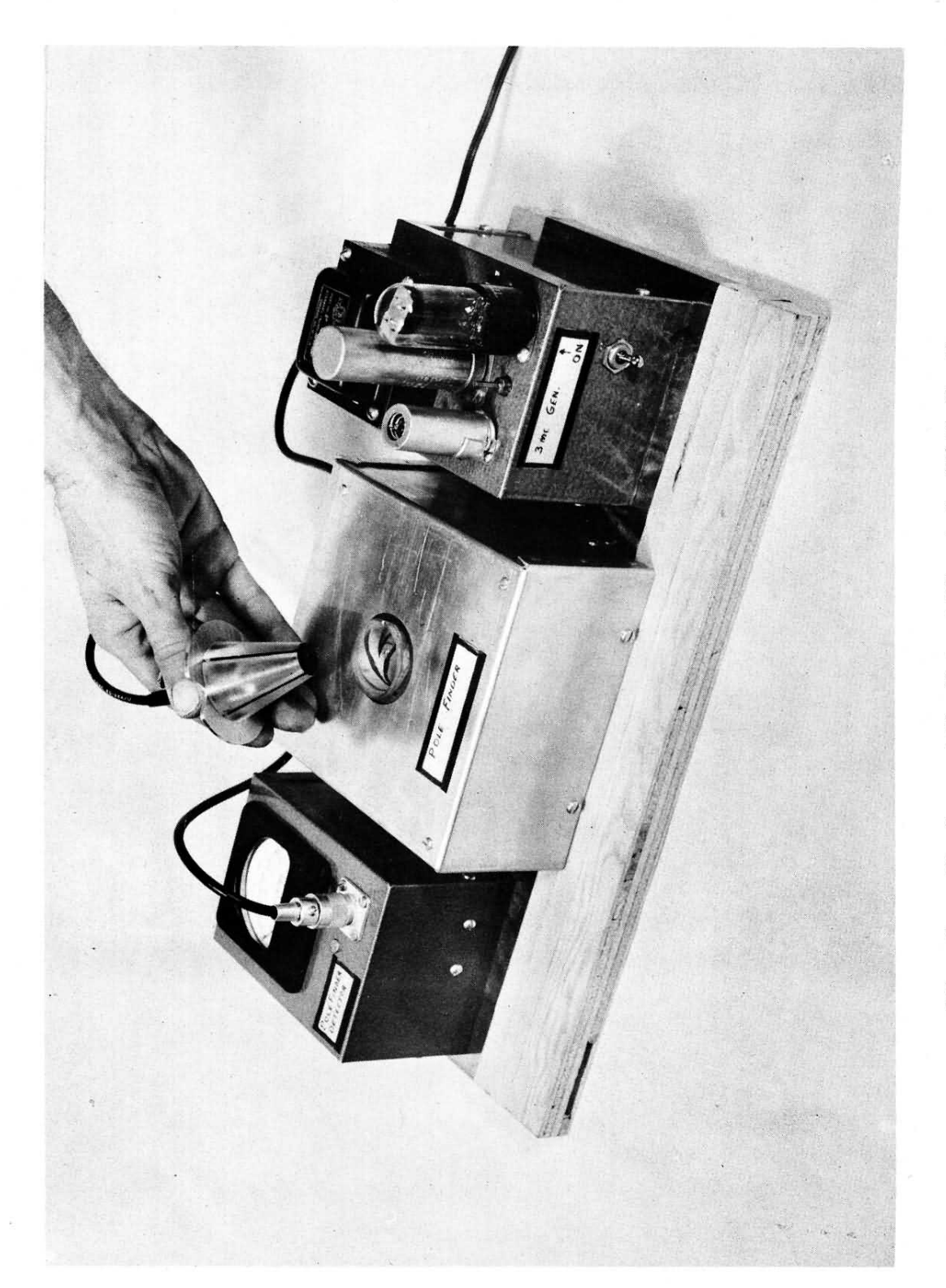


Fig. 3: Equipment To Detect The Axis Of Deflection In An Electro-Static Yoke.

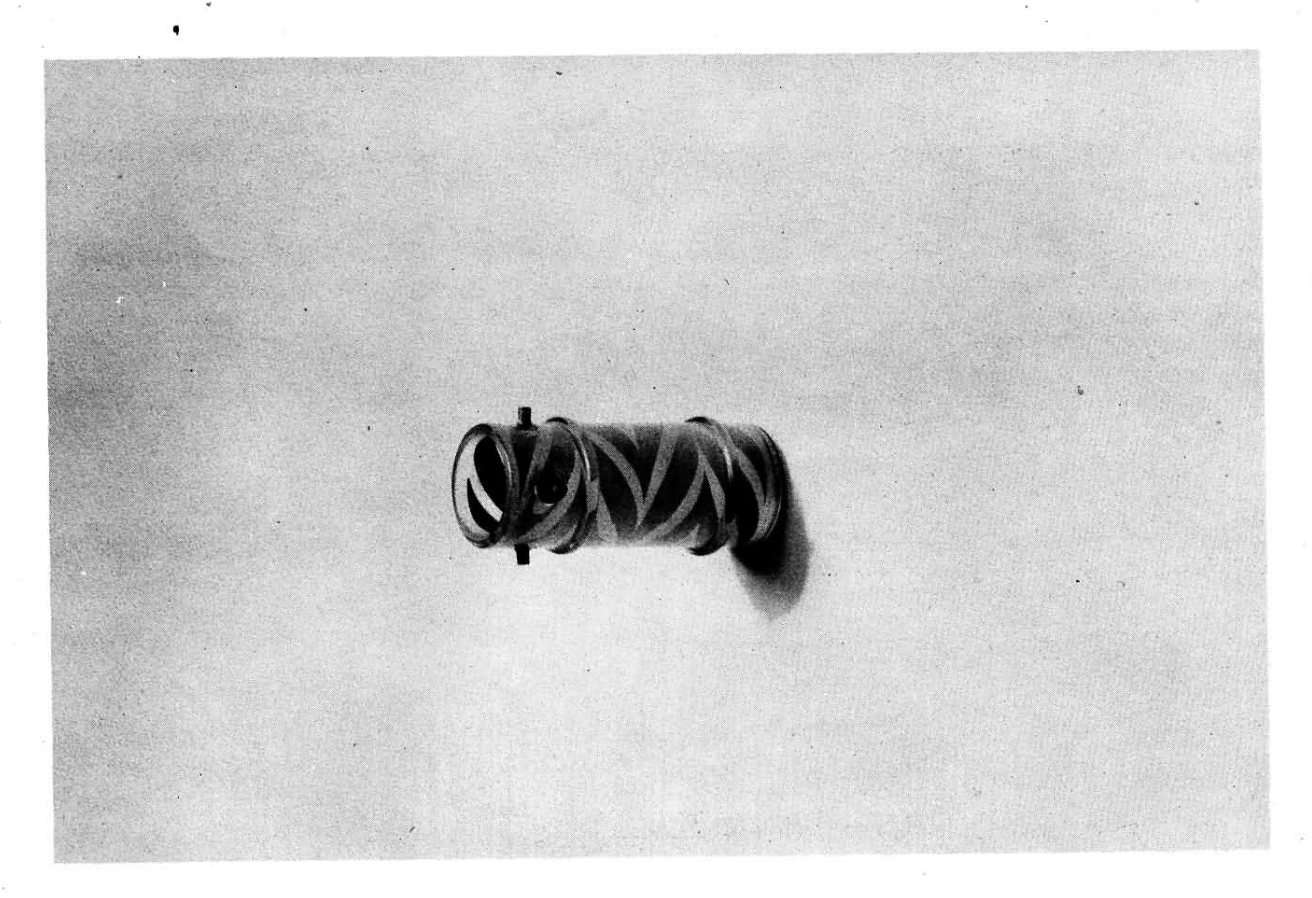


Fig. 4a: Narrow Angle Pencil Deflectron Type CY1-33.

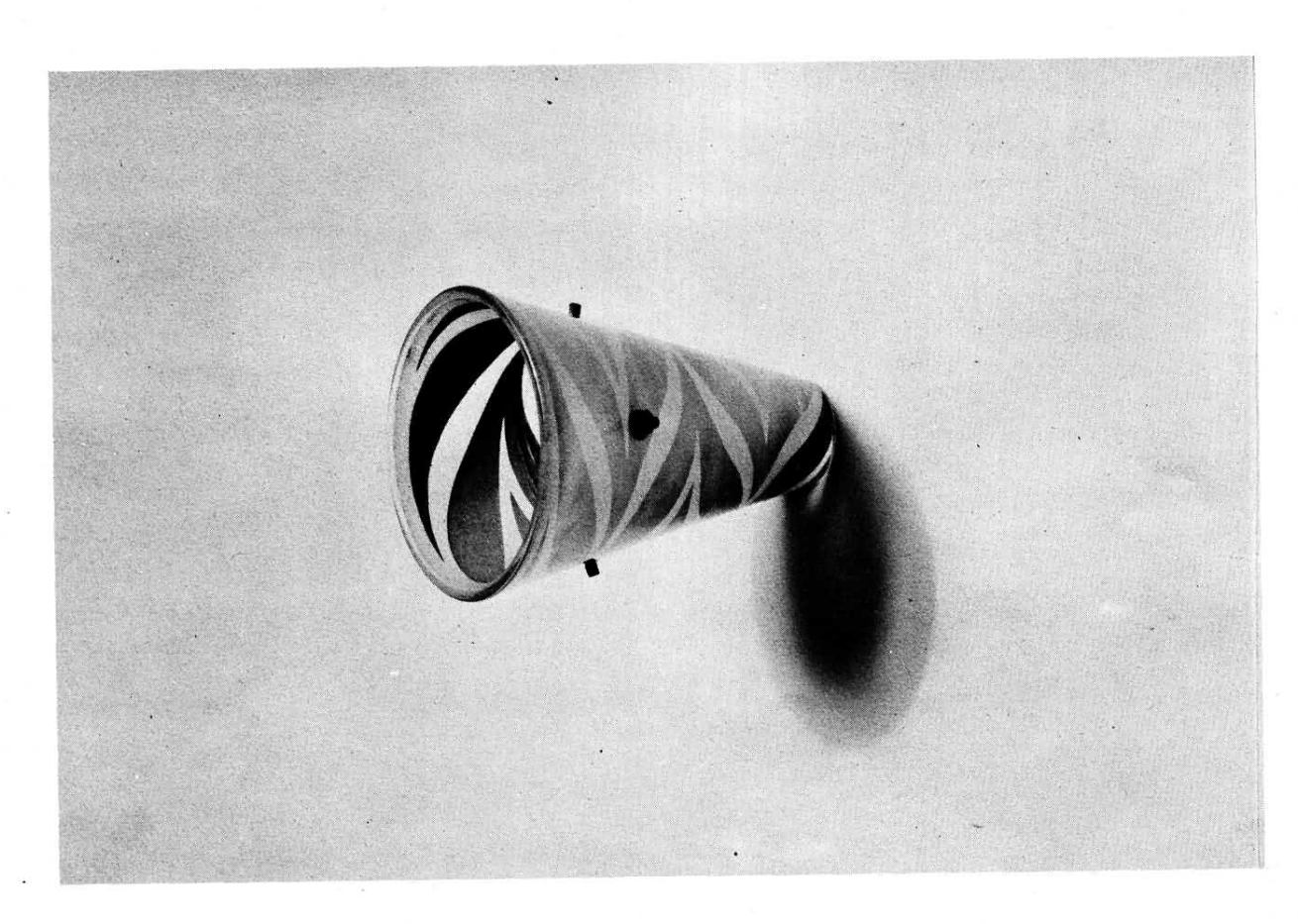


Fig. 4b: Wide Angle Deflectron Type C04-66.

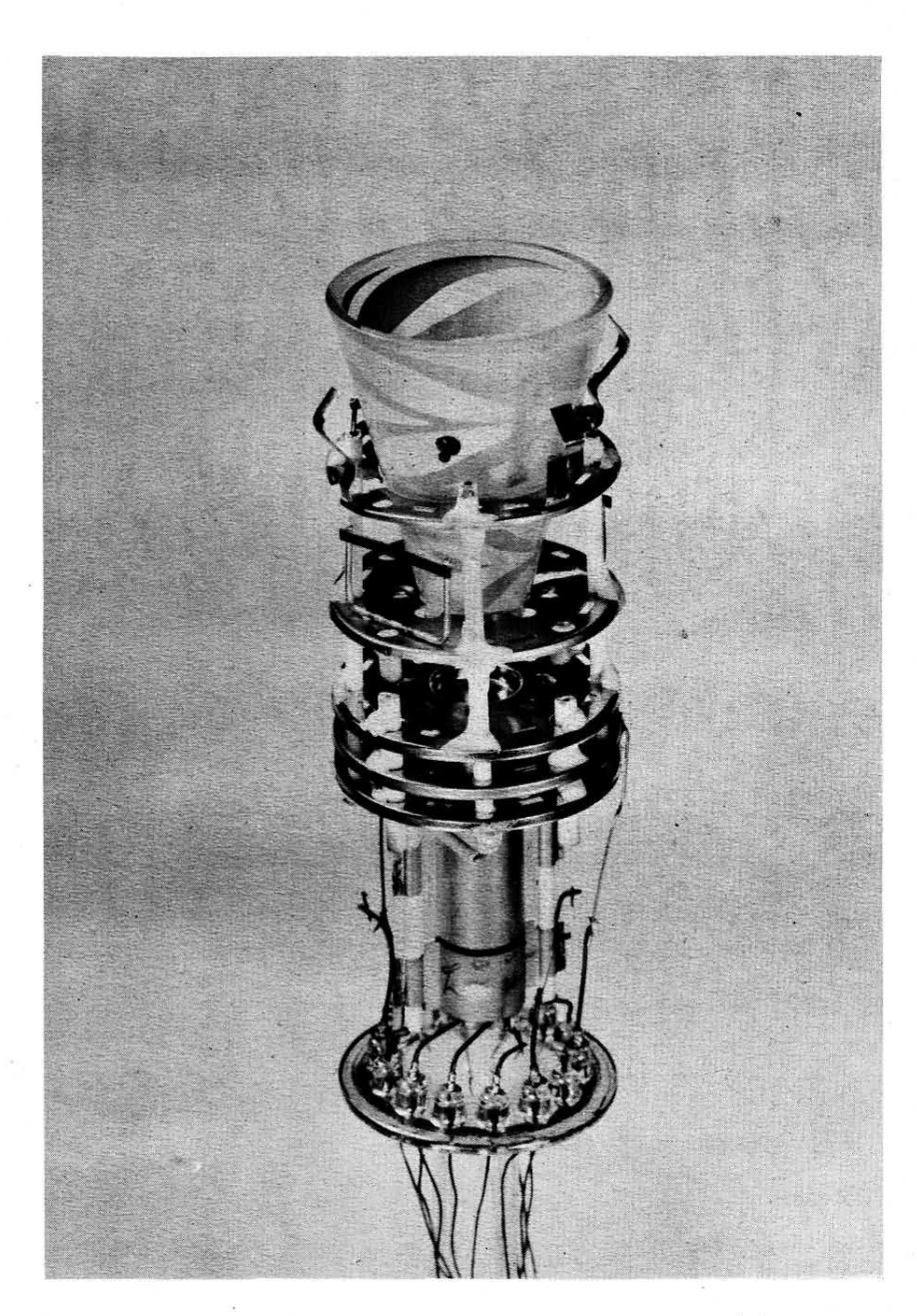


Fig. 5: Gun Assembly With Electro-Static Yoke.

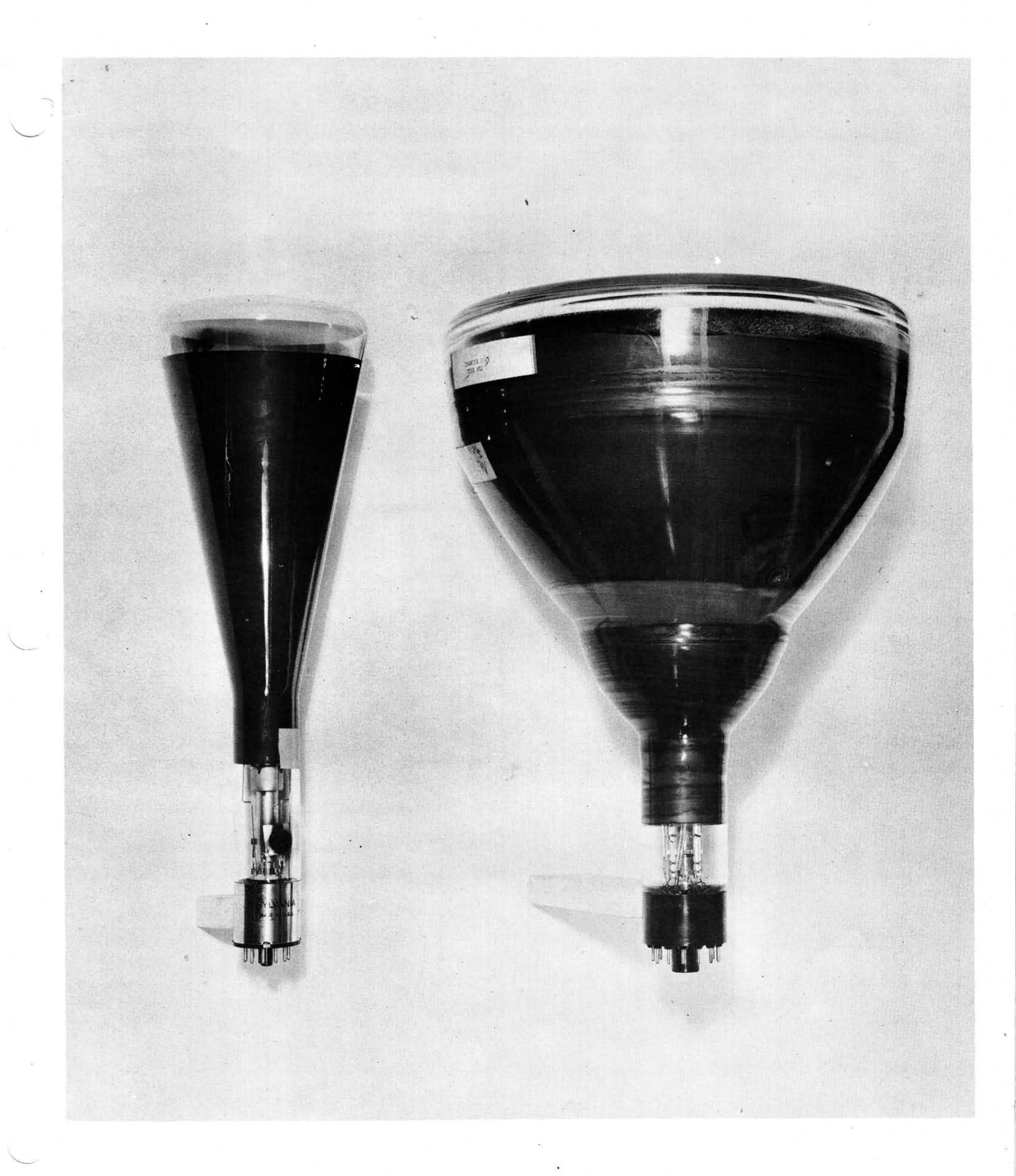


Fig. 6: 5-inch - 25 Degree Conentional Oscilloscope.

12-inch - 50 Degree Deflectron Tube Using Electro-Static Yoke.



Fig. 7: Optical Test Stand To Check Deflectron-Circularity.

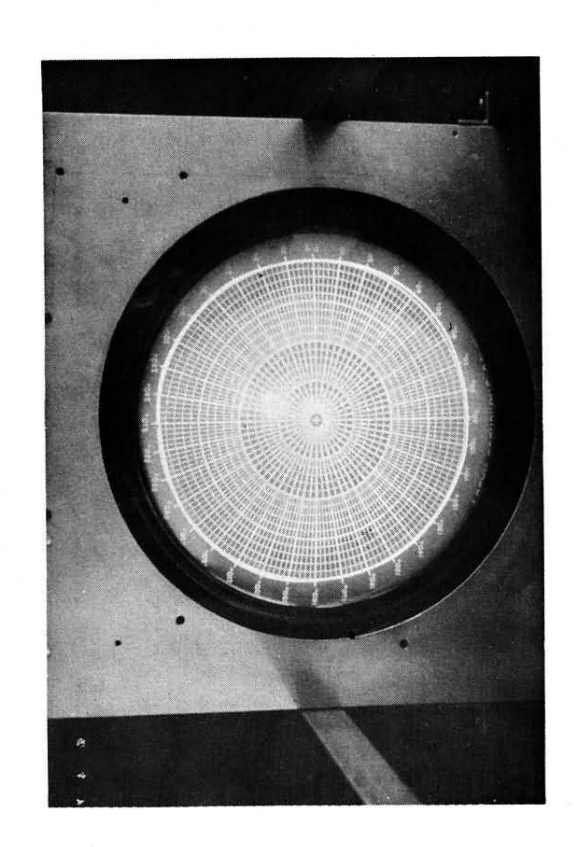


Fig. 8: Quadrantal Error Favoring Diagonals.

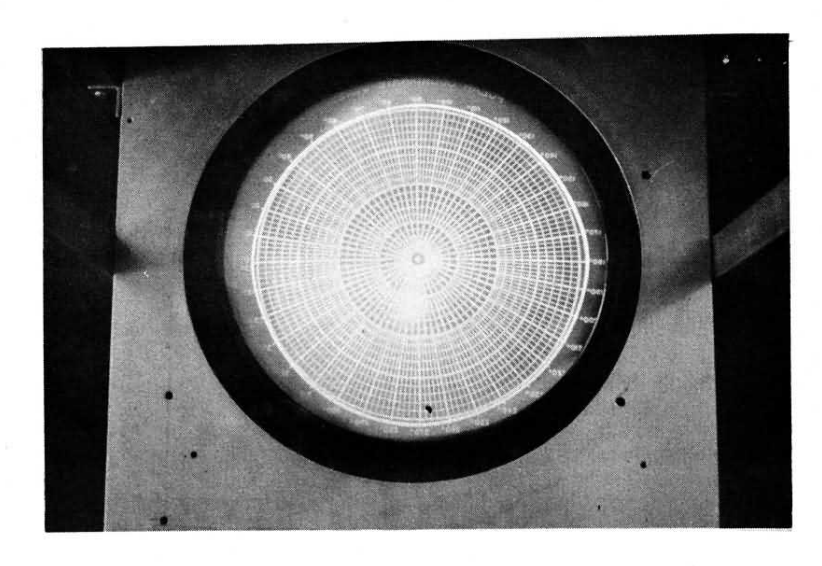
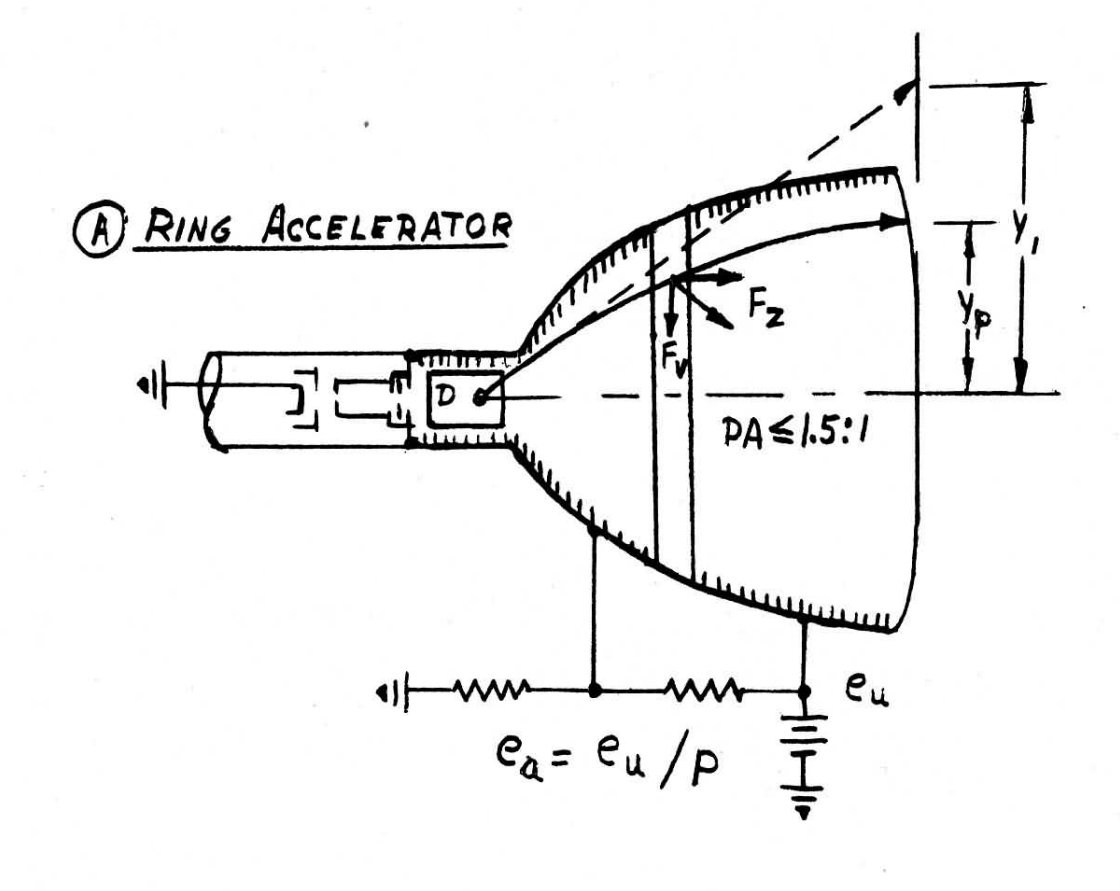


Fig. 9: Quadrantal Error Over Corrected Favoring Axials.



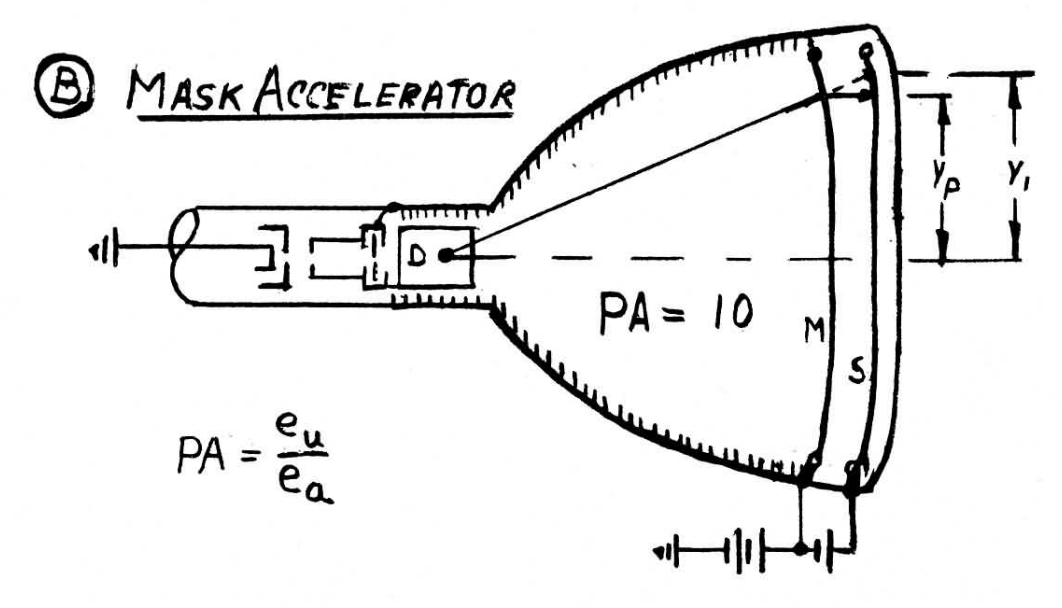


FIG. 10: Two Types OF INTENSIFIERS

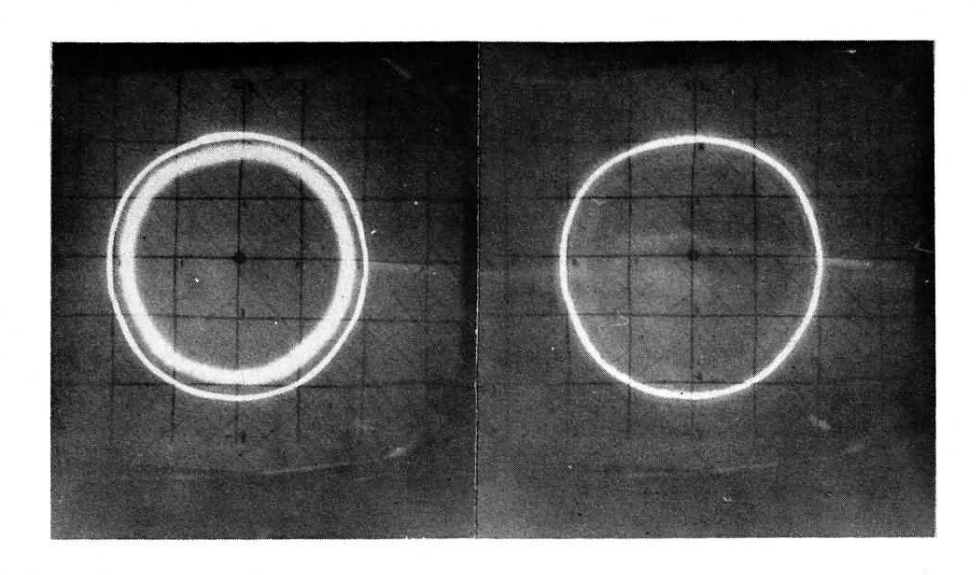


Fig. 11: Barrier Mask Intensifier:

a) Barrier Bias Removed
Secondary Image Appears
b) Barrier Mask In Operation

K CATHODE

G1 CONTROL GRID

A, 1 ST. ANODE

A2 2 ND ANODE

F FOCUSSING CYLINDER

D1-4 DEFLECTRON

M BARRIER MASK

S METAL-BACK SCREEN

TYPICAL OPERATION $B = 72^{\circ}$ P = 10:1 Post-Recleration $C_{u} = 20 KV$ $C_{z} = 2 KV$ $C_{p} = 1.9 KV$ $C_{p} = 1300 V P-P PER PLATE$

1.00 × Eu -/80/-0 < 6 < 400v **©**

FIG. 12: CRT. WITH ELECTROSTATIC YOKE AND BARRIER-MASK INTENSIFIER